Symbiosis

www.symbiosisonline.org
www.symbiosisonlinepublishing.com

Review Article | Nanoscience & Technology: Open Access | Open Access

# Evolution of Microstructure and Exchange Bias Characteristics of $NiFe_2O_4$/NiO nanocomposite

**P. Mallick***

*Department of Physics, North Orissa University, Takatpur, Baripada, Odisha, India.*

**Received: November 02, 2016; Accepted: November 10, 2016; Published: November 15, 2016**

***Corresponding author:** Department of Physics, North Orissa University, Takatpur, Baripada, Odisha, India, pin-757003, Tel: +91 9437656274 ; E-mail: pravanjanphy@gmail.com*

## Abstract

The occurrence of exchange bias (EB) characteristics in the systems attracted research attention owing to their application possibilities. This review highlights the effect of various parameters on the evolution of microstructure and exchange bias characteristics of $NiFe_2O_4$/NiO nanocomposite. The microstructure of $NiFe_2O_4$ present in $NiFe_2O_4$/NiO nanocomposite is strongly influenced by the synthesis methods as well as the synthesis conditions. The influence of various parameters like field cycle, molar ratio, size, temperature etc. on the EB characteristics is discussed. For the occurrence of good EB characteristics with promising application potentiality one need to synthesize the system avoiding the formation of relatively larger size $NiFe_2O_4$ particles or more ferromagnetic $NiFe_2O_4$ phase in the system.

**Keywords**: Nanocomposite, Exchange Bias, Inorganic compound, Magnetic properties, $NiFe_2O_4$

## Introduction

In recent years, $NiFe_2O_4$ has attracted considerable research attentions due to its diverse possible technological application possibilities in microwave devices [1], magnetic drug delivery [2], magnetic high-density data storage [3], catalysis [4, 5], radio-frequency range [6], hyperthermia [7], gas sensing [8], humidity sensing [9] etc. The reduction of the size from bulk to nanoscale optimizes the material properties regarding certain technological purposes in many of these applications as new phenomena arise due to enhancement of surface effect in the nanoscale regime [10].The study of the properties of magnetic nanoparticles is not only important from basic but also form technological point of view [11, 12]. In addition, the transition from single component to composite systems in the nanoscale regime offers great possibilities for tailoring the performance of the resultant composite [13]. The magnetic nanocomposites have attracted much attention in different fields due to their synergistic effect and magnetic exchange interactions. These nanocomposites opened up a new opportunity to develop the excellent multifunctional materials with their excellent magnetic properties [14].

Among the different well studied ferrite/metal oxide nanocomposites, $NiFe_2O_4$/NiO system has attracted considerable attention because of its excellent catalytic [15] and exchange bias (EB) characteristics [16-23]. The existence of EB coupling in this system demands its potentiality for designing permanent magnet [24-26] as well as other various applications like data storage (M-RAM), microelectronics (spin and tunneling valves), magnetic sensors (read/write heads), and medicine (drug delivery) [27, 28].

In this work, we review the effect of different conditions on the microstructure and exchange bias characteristics of $NiFe_2O_4$/NiO nanocomposite.

## Synthesis Methods

There are several methods available in the literature for the synthesis of $NiFe_2O_4$/NiO nanocomposite in power and thin film form. Yanqing et al., [29] synthesized $NiFe_2O_4$/NiO by calcining the ball milled product of the initial ingredient of NiO and $Fe_2O_3$. One can used chemical co-precipitation and post thermal decomposition [16, 17, 20-23] to obtain $NiFe_2O_4$/NiO nanocomposites. $NiFe_2O_4$/NiO nanocomposites have also been synthesized by the thermal treatment of NiFe-layered double hydroxides [19].NiO nanoparticles can be implanted into $NiFe_2O_4$ nanowires chemically to prepare ordered NiO/$NiFe_2O_4$ nanocomposites [14]. One can also adopt the Gen's levitation jet method to synthesize NiO/$NiFe_2O_4$ composite [30, 31]

$NiFe_2O_4$/NiO composite coating can be synthesized by heat treating the electroplated Ni–Fe alloy [32]. Thin films of $NiFe_2O_4$/NiO were also synthesized using high-pressure microplasma-based deposition [33].

Among the different method, chemical co-precipitation and post thermal decomposition method has been adopted in most of the studies.

## Evolution of Microstructure of $NiFe_2O_4$

The crystal structure of $NiFe_2O_4$ is not affected by varying the synthesis conditions. However, the microstructure of $NiFe_2O_4$ is

strongly influenced by the synthesis conditions. For example: (i) by changing the precursor or solvent in a similar procedure, (ii) by changing the synthesis method using the same precursor. Other parameters like sintering temperature, sintering time etc. also play the crucial role in controlling the microstructure of the $NiFe_2O_4$. The evolution of microstructure of $NiFe_2O_4$ under different synthesis conditions are discussed in the followings.

## Effect of Synthesis Method

Zhao et al. [19] synthesized $NiFe_2O_4$/NiO nanocomposite from a nickel iron layered double hydroxide (NiFe-LDH) precursor and by the chemical co-precipitation method. These authors have seen that the calcination of NiFe-LDH precursor at 500 $^0$C led to the development of $NiFe_2O_4$ is ~ 6 nm in the $NiFe_2O_4$/NiO nanocomposite. These authors also reported the formation of 20 nm size crystallite of $NiFe_2O_4$ by the calcination of the precursor synthesized by the chemical co-precipitation method at 500 °C. The crystallite size of the $NiFe_2O_4$ obtained by co-precipitation method is about three times that of the material prepared using the LDH precursor method. Ma et al. [32] synthesized $NiFe_2O_4$/NiO composite by thermal oxidation of electroplated Ni–Fe alloy. These authors have reported the formation of homogeneously distributed dense and flat structure of $NiFe_2O_4$ in the matrix of NiO.

Pebley et al. [33] have synthesized nanostructured $NiFe_2O_4$/NiO films using high-pressure microplasma-based deposition by varying Ni molar compositions ($x_{Ni}$). These authors reported that the presence of both $NiFe_2O_4$ and NiO in the samples prepared with $x_{Ni}$ = 0.49–0.74. From the elemental mapping of Fe and Ni, these authors suggested that 50–100 nm size $NiFe_2O_4$ crystals are dispersed in a matrix of larger ~100–200 nm NiO grains.

It is clear from the above comparison that the size of $NiFe_2O_4$ is being influenced by changing the synthesis method.

## Effect of Initial Precursor

It has been seen that the changing the initial precursor for the synthesis in a particular synthesis procedure influences the microstructure like crystallite size of the material. Even with the same initial precursor with a slightly modification in the synthesis condition also affect the crystallite size of the material. Tian et al. [16] and He et al. [18] have synthesized $NiFe_2O_4$/NiO nanocomposite by co-precipitation method using different initial precursor and these authors have obtained different crystallite size of $NiFe_2O_4$ (Table 1). Gong et al. [21] have used same initial precursor and adopted same synthesis method as used by Tian et al. [16] but due to slight modification in both their synthesis condition led to the formation of different size $NiFe_2O_4$ (Table 1).

## Effect of Calcination/Sintering Temperature and Time

Zhao et al. [19] also synthesized $NiFe_2O_4$/NiO nanocomposite using NiFe-LDH precursor with Ni/Fe molar ratio ~ 3. These authors calcined the NiFe-LDH precursor at 500 $^0$C and seen that the crystallite size of $NiFe_2O_4$ is ~ 6 nm. In an another work, Zhang et al. [34] also synthesized $NiFe_2O_4$/NiO nanocomposite NiFe–LDH precursor and obtained 44.73 nm size crystallites of $NiFe_2O_4$ in $NiFe_2O_4$/NiO nanocomposite by calcined the NiFe–LDH precursor (with a Ni/Fe molar ratio ~ 3) at 900 $^0$C for 4 hours.

Tian et al. synthesised $Ni_{1-x}Fe_xO$ ($x$ = 0.09) by co-precipitation method [17] and subjected the Fe doped NiO product to high temperature sintering [22]. These authors have studied the effect of sintering temperature and time on the microstructural property of the material [23]. The evolution of crystallite size of NiO and $NiFe_2O_4$nanoparticles with sintering temperature is presented in Table 2. As indicated from the table (2) that crystallites size of $NiFe_2O_4$ increases 0 to 55 nm with increasing sintering temperature from 550 to 1000 $^0$C (Figure. 1).Fitting the variation of crystallite size ($D$) of $NiFe_2O_4$with sintering temperature ($T$) to linear fit (Figure. 1) indicated that the size of $NiFe_2O_4$increases linearly with the sintering temperature following the relation:

$$D = 0.12113 \times T - 65.30625 \quad (1)$$

The size of the crystallites of $NiFe_2O_4$ sintered at 600 $^0$C also shown to increase from 3 nm to 8 nm with increasing sintering time from 1 to 3 hours (Table 2).

## Effect of Molar Ratio

He et al. [18] synthesized $Ni_{1-x}Fe_xO$ (x = 0.15, 0.2, 0.3 and 0.5) bulk samples obtained using co-precipitation method

**Table 1**: $NiFe_2O_4$ nanoparticles with different size present in $NiFe_2O_4$/NiO nanocomposite synthesized in a same method using different initial precursors

| Sl. No. | Synthesis Method | Initial Precursor/ Sample | Solvent | Size (nm) of $NiFe_2O_4$ | References |
|---|---|---|---|---|---|
| 1 | Co-precipitation method | $NiCl{\cdot}6H_2O$, $FeCl_3{\cdot}6H_2O$, $NH_4HCO_3$ | Distilled Water | 8 | Tian et al. [16] |
| 2 | Co-precipitation method | $Ni(NO_3)_2.6H_2O$, $Ni(NO_3)_3.9H_2O$, $NH_4HCO_3$ | Distilled Water | 20 | He et al. [18] |
| 3 | Co-precipitation method | $NiCl{\cdot}6H_2O$, $FeCl_3{\cdot}6H_2O$, $NH_4HCO_3$ | Distilled Water | 12 | Gong et al. [21] |

**Table 2**: Variation of crystallite size of NiO and $NiFe_2O_4$ present in $Ni_{1-x}Fe_xO$ ($x$ = 0.09) sintered at different temperature [Reprinted from Tian Z et al. J. Appl. Phys. 2014; 115(8): 083902 [23], with the permission of AIP Publishing].

| Sintering Temperature ($^0$C) | Sintering Time (h) | Crystallite Size of NiO (nm) | Crystallite Size of $NiFe_2O_4$ (nm) |
|---|---|---|---|
| 550 | 3 | $10 \pm 1$ | 0 |
| 600 | 1 | $15 \pm 1$ | $3 \pm 1$ |
| 600 | 3 | $20 \pm 2$ | $8 \pm 1$ |
| 650 | 3 | $32 \pm 5$ | $12 \pm 2$ |
| 700 | 3 | $60 \pm 5$ | $22 \pm 2$ |
| 800 | 3 | $85 \pm 5$ | $32 \pm 2$ |
| 1000 | 3 | $140 \pm 5$ | $55 \pm 3$ |

and annealed at 650 $^0$C for 12h in order to get $NiFe_2O_4$/NiO nanocomposite. These authors have reported the formation of 20 nm size $NiFe_2O_4$ nanoparticles in $NiFe_2O_4$/NiO nanocomposite. Gong et al. [21] have synthesized (100-x)NiO/(x)$NiFe_2O_4$ nanocomposites with x= 0, 2.5, 5, 8.3, 12.5, 25 were prepared by a chemical co-precipitation method followed by sintering at 600 $^0$C for 3h. They have reported that all the samples show an average particle sizes of 12 nm with the formation of $NiFe_2O_4$/NiO nanocomposite for x>2.5.

## Evolution of Magnetic Properties of $NiFe_2O_4$ present in $NiFe_2O_4$/NiO

The occurrence of different types of magnetic ordering of $NiFe_2O_4$ present in $NiFe_2O_4$/NiO is discussed in the followings.

### Ferromagnetic property

He et al. [18] obtained $NiFe_2O_4$/NiO nanocomposite by annealing $Ni_{1-x}Fe_xO$ (x = 0.15, 0.2, 0.3 and 0.5) synthesized by co-precipitation method. Their temperature dependent of field cooled magnetization measured at a field of 1 kOe indicated the occurrence of ferromagnetic type magnetization in all samples. Their study further indicated that the existence of the effective exchange coupling interface between NiO and $NiFe_2O_4$. In another work, Zhang et al. [34] also have reported the occurrence of ferromagnetic behaviour in $NiFe_2O_4$/NiO nanocomposite synthesized by using NiFe-LDH precursor.

### Superparamagnetic property

Zhao et al. [19] reported the the occurrence of superparamagnetism $NiFe_2O_4$/NiO nanocomposite synthesized by using NiFe-LDH precursor and co-precipitation method. Their zero field cool (ZFC) and field cool (FC) magnetization of the samples measured at an applied field of 100 Oe indicated the sample prepared using NiFe-LDH precursor having 6 nm size $NiFe_2O_4$ nanoparticles show the blocking temperature ($T_B$) of 380 K whereas the $T_B$ is ~280 K for the sample prepared using co-precipitation method having 20 nm size $NiFe_2O_4$ nanoparticles. Their study indicated:

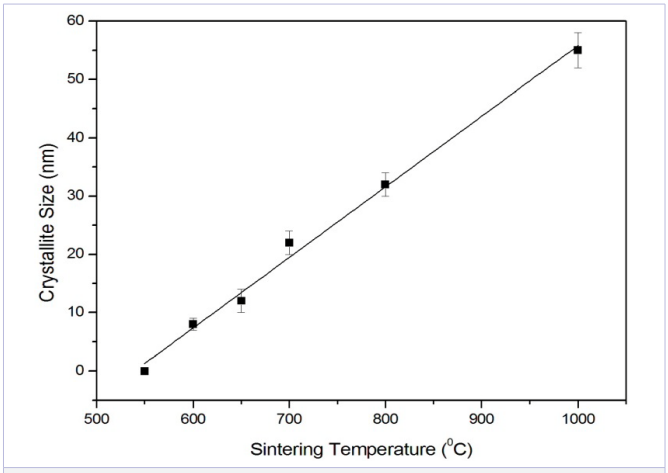


**Figure 1:**Variation of crystallite size of $NiFe_2O_4$ in $Ni_{1-x}Fe_xO$ ($x$ = 0.09) sintered at different temperaturefor 3 hours (Data taken from the ref. [23]). Line represents the linear fit to the data points.

(i) the occurrence of higher value of $T_B$ than the single phase Ni-$Fe_2O_4$ nanoparticles with size < 10 nm [35, 36], (ii) the coupling of NiO and $NiFe_2O_4$ could be a source of enhanced magnetization stability as a result of which $T_B$ increased.

### Spin glass Property

Tian et al. [16, 22] studied the effect of annealing on magnetic behaviour of $NiFe_2O_4$/NiO nanocomposite. Their magnetization characterization indicated that the saturation magnetization of all the samples increase with increasing annealing temperature. The coercivity on the other hand follows a nonmonotonic size dependencies and show the maximum value for the sample with 15 nm size $NiFe_2O_4$ nanoparticles.These authors pointed out that the nonmonotonic behaviour of coercivity could be due to the variation of total anisotropy arise from the contribution of $NiFe_2O_4$ cores and the interfacial exchange coupling energy [37, 38]. Their ZFC and FC magnetization indicated that the ZFC and FC magnetization curves diverge below certain temperature called irreversibility temperature. The divergences become smaller with increasing the size of $NiFe_2O_4$ nanoparticles and both the curve fully coincides for sample with size of $NiFe_2O_4$ nanoparticles is above 32 nm. These authors also have seen that the peak of ZFC magnetization curves shifts to lower temperatures, correlated with the reduction of magnetic disorder at interfaces [22].

In order to understand the low temperature magnetic behaviour of the samples, these authors [22], undertaken temperature dependent ZFC and FC magnetization at various magnetic fieldfor sample with 8 nm size $NiFe_2O_4$ nanoparticles. Their study indicated that the occurrence of spinglass phase due to the existence of intermediate structural disordered layers at $NiFe_2O_4/Ni_{1-x}Fe_xO$ interfaces [16, 22].

### Exchange bias (EB) effect in $NiFe_2O_4$/NiO

In 1956, the phenomenon of exchange bias (EB) was discovered by Meiklejohn and Bean [39] in ferromagnetic (FM) Co particles coated antiferromagnetic (AFM) CoO which referred to the shift of a hysteresis loop along the magnetic field axis.In order to generate EB effect, there must be the co-existence of two phases i.e. one with net magnetic moment whose magnetic moment can be reversed and other phase which can exert a torque action on the spins of the former during the process of magnetization reversal [22, 28, 40]. Since its discovery, EB effect has also been studied in other systems like ferrimagnetic (FiM) coupled with other (AFM or FM) [41, 42] or spinglass (SG) coupled with other (FM, AFM orFiM) [28, 43, 44]. In recent years, EB in nanoparticle systems has attracted much attention because of the unique properties of nanoparticles and their potential technological applications [45].In contrast to bilayer systems, the inclusion of FM cluster in AFM matrix is interesting from fundamental point of view [22].

The phenomenon of EB in the system is quantified by calculating EB field, $H_{EB}$ as

$$H_{EB} = -\frac{H_{C1} + H_{C2}}{2} \qquad (2)$$

and the coercivity, $H_C$ as

$$H_C = \frac{H_{C2} - H_{C1}}{2} \quad (3)$$

where $H_{C1}$ and $H_{C2}$ are the left and right coercive field, respectively [46, 47]. The vertical magnetization shift ($M_{Shift}$) is also calculated by taking the difference of saturation magnetization between the measured hysteresis loop and the loopcentered in the M axis [22].

In this section, we discuss the EB effect of $NiFe_2O_4$ nanoparticles embedded in NiO matrix. There are several effects like field cycle, molar ratio, size, temperature etc. which affects the EB in the system are discussed in the followings.

## Effect of Cooling Field

Tian et al. studied the effect of cooling field on the EB characteristics of $NiFe_2O_4$ nanoparticles embedded in NiO matrix [16]. Their study indicated that the $H_{EB}$ increases with increasing cooling field from 0 to 12 kOe and the same saturates thereafter. These authors argued that only a part of spins at the Ferri/AFM interface are pinned along the cooling field direction for smaller fields and more spins are pinned along the field direction which causes the enhancement of exchange interaction with increasing cooling field. As a result of which $H_{EB}$ increases with increasing cooling field. For higher cooling field (>12 kOe), the pinned spins along the field saturates which resulted into the saturation of $H_{EB}$.

## Effect of Field Cycle

Tian et al. [17] studied the effect of field cycle on the EB characteristics of $NiFe_2O_4$ nanoparticles embedded in NiO matrix. Their study indicated that both $H_{EB}$ and $M_{Shift}$ decrease with the increasing field cycling [17].

## Effect of Cycle Dependent Cooling Field

In another work, Tian et al. studied the effect of cycle dependent cooling field on the EB characteristics of $NiFe_2O_4$ nanoparticles embedded in NiO matrix [20]. Their study indicated that the $H_{EB}$ increases with increasing cooling field for a particular cycle and the relative change in $H_{EB}$ i.e. $H_{EB}$ decreased by ~ 71% from its initial value for cooling field at 0Oe whereas the same decreased by 54% for cooling field at 40 kOewith increasing loop cycle to $n$ = 9 [20]. These authors argued that decrease of $H_{EB}$with increasing loop cycle reflects the configurational rearrangements of the spin structure and can be expressed by the following discretized Landau-Khalatnikov equation [48, 49]:

$$H_{EB}(n+1) - H_{EB}(n) = -\gamma\left[H_{EB}(n) - H_{E\infty}\right]^3 \quad (4)$$

Where $H_{E\infty}$ and $\gamma$ are fitting parameters which describe $H_{EB}$ vs. $n$ in the limit of infinite loops and the characteristic decay rate of the training behavior, respectively. The monotonic decrease of $\gamma$ with increasing cooling filed in case of Tian et al. [20] also confirm the reduction of training effect for high cooling field. The authors assumed the coexistence of the two possible mechanism on training effect [50] to their case i.e. (i) FM magnetization is in a multi-domain state for $H_{EB}$ = 0 Oe, which reverses via a symmetric mechanism, and can lead to the suppression of training effect, (ii) higher field cooling results in a single-domain state, asymmetric reversal process via domain wall and nucleation process take place which led to larger training effect.

## Effect of Size Dependent Field Cycle

In order to see the size dependent field cycle effect on EB characteristics, Tian et al. [23]studied the variation of normalized $H_{EB}$ and normalized coercivity enhancement ($\Delta H_C$) as a function of different size of $NiFe_2O_4$ nanoparticles embedded in NiO matrix. Their result indicated that both the parameter decrease with increasing size of $NiFe_2O_4$with a minima for the sample with 22 nm size $NiFe_2O_4$ nanoparticles. The suppression of normalized $H_{EB}$ and $\Delta H_C$ by 75% and 82% respectively for the sample with 22 nm size $NiFe_2O_4$ nanoparticles indicated the correlation between $H_{EB}$ and $\Delta H_C$ as seen for other systems [51, 52]. The reduction in $H_{EB}$ could be due to the weakening of interfacial exchange coupling energy due to the depinning of frozen AFM spins and the loss of interfacial coupling energy between FM/ AFM system after each field cycle. Further, the slower change in $H_{EB}$ for larger particle size could be due to enhancement of the interfacial coupling stiffness for larger AFM particles which leads to relatively smaller interfacial energy losses after each field cycle [23].

## Effect of Molar Ratio

**Effect of $NiFe_2O_4$ ratio:** Gong et al. [21] synthesized (100-x) NiO/(x)$NiFe_2O_4$ nanocomposites by varying x(x= 0, 2.5, 5, 8.3, 12.5, 25) by a chemical coprecipitation method. These authors pointed out that $NiFe_2O_4$ has not been detected by XRD for the composite sample with x=2.5. For x concentration > 2.5, both antiferromagnetic NiO and ferrimagnetic $NiFe_2O_4$ coexist in the nanocomposites. These authors calculated the average particle size as 12 nm for all the samples from XRD line width using Scherrer formula [53] which agree with their TEM observation. Their study indicated that the $H_{EB}$ for pure NiO (i.e. with x=0) is 1.1 kOe which increases with increasing x concentration i.e. concentration of $NiFe_2O_4$ up to x = 2.5 and the same decreases with further increasing x concentration.The observation of $H_{EB}$ for pure NiO is attributed to the exchange coupling between the spins of the AFM core and the uncompensated surface moments of NiO nanoparticles [54-56]. The large loop shift and coercivity observed in AFM nanoparticles is a consequence of the transition from two-sublattice to multisublattice of the AFM NiO nanoparticles [44, 57]. It has been reported that the$H_{EB}$ and $H_C$ decrease with increasing temperature in AFM/FM or AFM/FI systems because the excess thermal energy decreases the exchange coupling between AFM/FM and AFM/FI [58]. The strong interfacial exchange coupling between NiO and $NiFe_2O_4$ is the cause for the increase of $H_{EB}$ with increasing $NiFe_2O_4$ concentration up to x = 2.5 [16]. Hence, the authors suggested that nanocomposite with x=0.25 is the percolation threshold of the nanocomposites which further confirms the observation of He et al. [18] that the presence of more $NiFe_2O_4$ phase in NiO or the formation of isolated $NiFe_2O_4$ in the composite for x>2.5 reduces the interface coupling between NiO and $NiFe_2O_4$ as a result of which $H_{EB}$ decreases in the samples. Similar type of

behaviour has also been reported for Ni/NiO [59] and $NiFe_2O_4$/NiO [14] nanocomposites.

**Effect of Fe concentration in $Ni_{1-x}Fe_xO$:** He et al. [18] synthesized $Ni_{1-x}Fe_xO$ with different Fe concentration by co-precipitation method and finally annealed the samples at 650$^0$C for 12 hours. In order to study the effect of Fe concentration of the EB characteristics of the samples, the authors calculated $H_{EB}$ as a function of temperature for the samples with different Fe concentrations from M-H curve of the samples taken by cooling the sample at an applied field of 1kOe from 300K. These authors reported that the value of $H_{EB}$ decreases with increasing the Fe content x at the same temperature. These authors argued that the enhancement of ferromagnetic type interactions among $NiFe_2O_4$ particles with increasing Fe content could be the cause of suppression of $H_{EB}$.

**Effect of Ni/Fe molar ratios:** Zhao et al. [19] synthesized different $NiFe_2O_4$/NiO nanocomposites by calcining NiFe-LDH-LDH precursors with different $Ni^{II}/Fe^{III}$molar ratios at 500 $^0$C. These authors have seen that the value of $H_{EB}$ increased from 53.6 Oe to 330.4 Oe with increasing $Ni^{II}/Fe^{III}$ molar ratios from 2:1 to 4:1. This study further confirms the suppression of $H_{EB}$ with increasing size or fraction of $NiFe_2O_4$ phase in $NiFe_2O_4$/NiO as was seen by He et al. [18].

In another work, Pebley et al., [33] synthesized $NiFe_2O_4$/NiO nanocomposites by varying Ni molar fraction and studied the EB characteristics of the samples with Ni molar fraction. These authors reported that both $H_C$ and $H_{EB}$ under FC condition increase with increasing Ni molar fraction in the sample. This is in accordance with the previous observations that the interfacial density between the $NiFe_2O_4$ and NiO phases increases with increasing Ni content.

## Effect of Sintering Temperature

In order to understand the suppression of $H_{EB}$ with increasing Fe content as discussed above, He et al. [18] also undertaken the effect of sintering temperature which resulted into larger size $NiFe_2O_4$ particles in $NiFe_2O_4$/NiO with increasing sintering temperature. Their study indicated that the $H_{EB}$ of the sample decreases with increasing sintering temperature and the $H_{EB}$ nearly vanishes for the sample sintered at 850 $^0$C for 12 hours. With increasing sintering temperature, the size of particles become larger and the $NiFe_2O_4$ particles may form ferromagnetic type clusters in NiO matrix as result of which effective coupling among the $NiFe_2O_4$ and NiO decreases. Similar types of observations have also been reported [19, 33, 60-62]. Hence it is clear from the study that relatively larger size $NiFe_2O_4$ particles or more ferromagnetic $NiFe_2O_4$ phase in the system is not the good choice for the occurrence of EB in this system.

In another work, Tian et al. [22] sintered their sample at various temperatures to investigate the $NiFe_2O_4$ size dependent $H_{EB}$ of $NiFe_2O_4$/NiO. The authors have seen that the size of $NiFe_2O_4$ increasedfrom 0 to 55 nm with increasing sintering temperature from 550 to 1000 $^0$C (Figure 1). The authors also sintered the same sample at 600$^0$C for 1 hour to get the sample with ~ 3 nm size $NiFe_2O_4$ particles. Their study of temperature dependent $H_{EB}$ and $M_{Shift}$ indicated that the EB field decreases with increasing temperature and vanishes above 250 K for all samples (i.e. irrespective of crystallite size of $NiFe_2O_4$) and the same decreases rapidly for the sample with smaller size ($\leq$ 12 nm) $NiFe_2O_4$.The variation of $M_{Shift}$ with temperature is in agreement with the variation of $H_{EB}$ for smaller size $NiFe_2O_4$ particles. However, no similar variation in both the parameters are shown for samples with size $NiFe_2O_4$ particles > 22 nm. In order to understand this behaviour, the authors plotted $H_{EB}$ vs. $M_{Shift}$ for samples with different size of $NiFe_2O_4$ particles. Their results indicated that the existence of linear relationship between $H_{EB}$ and $M_{Shift}$ for the samples with size of $NiFe_2O_4$ particles $\leq$ 8 nm indicated the correlation among them. The existence of linear dependency hence EB could be due to the coupling between the ferrimagnetic phase and the spin glass like phase formed due to structural disorder at the interface. The authors also pointed out that the open and unsaturation of field cooled loop measured at 10 K for sample with 8 nm size $NiFe_2O_4$ [16] further confirms the existence of spin glass like phase [60, 63]. The linear relationship between $H_{EB}$ and $M_{Shift}$ deviates for the sample with size of $NiFe_2O_4$ particles is ~ 12 nm and the same show two linear dependency for the sample with size of $NiFe_2O_4$ particles is ~ 22 nm. These authors [22] stated that the deviation of linear dependency could be due to coexistence of two interfacial exchange coupling: one is the exchange coupling between ferromagnetic $NiFe_2O_4$ core and the spinglass like layer related to the structural disorder region in $Ni_{1-x}Fe_xO$ nanoparticles and the other arise from the coupling of the $NiFe_2O_4$ phase and antiferromagnetic NiO phases.

## Conclusion

Effect of various parameters on the evolution of microstructure and exchange bias characteristics of $NiFe_2O_4$/NiO nanocomposite is reviewed. The microstructure of $NiFe_2O_4$ present in $NiFe_2O_4$/NiO nanocomposite is strongly influenced by the synthesis methods as well as the synthesis conditions. The effects of various parameters like field cycle, molar ratio, size, temperature etc. have been shown to affect the EB characteristics in the system. It is suggested through this study that relatively larger size $NiFe_2O_4$ particles or more ferromagnetic $NiFe_2O_4$ phase is not the good choice for the occurrence of EB in this system.

## References

1. Harris VG, Geiler A, Chen Y, Yoon SD, Wu M, Yang A, et al. Recent advances in processing and applications of microwave ferrites. J.Magn. Magn.Mater. 2009;321(14):2035-2047.

2. Yin H, Too HP and Chow GM. The effects of particle size and surface coating on the cytotoxicity of nickel ferrite. Biomaterials. 2005;26(29):5818-5826. DOI: 10.1016/j.biomaterials.2005.02.036

3. Wang Y, Teng X, Wang JS and Yang H. Solvent-free atom transfer radical polymerization in the synthesis of $Fe_2O_3$@ polystyrene core-shell nanoparticles. Nano Lett. 2003;3(6):789-793. DOI: 10.1021/nl034211o

4. Deraz NM, Alarifi A and Shaban SA. Removal of sulfur from commercial kerosene using nanocrystalline $NiFe_2O_4$ based sorbents. J. Saudi Chem. Soc. 2010;14(4):357-362. DOI: 10.1016/j.jscs.2010.04.012

5. Ren Y, Dong Q, Feng J, Ma J, Wen Q and Zhang M. Magnetic porous ferrospinel $NiFe_2O_4$: a novel ozonation catalyst with strong catalytic property for degradation of di-n-butyl phthalate and convenient separation from water. J.Colloid Interface Sci. 2012;382(1):90-96. doi: 10.1016/j.jcis.2012.05.053

6. Wang J. Prepare highly crystalline $NiFe_2O_4$ nanoparticles with improved magnetic properties.Mater. Sci. Eng. B. 2006;127(1):81-84.

7. Sang Won Lee, Seongtae Bae, Yasushi Takemura, In-Bo Shim, Tae Min Kim, Jeongryul Kim et al. Self-heating characteristics of cobalt ferrite nanoparticles for hyperthermia application. J. Magn. Magn.Mater. 2007;310(2):2868-2870.

8. Reddy CG, Manorama SV and Rao VJ. Preparation and characterization of ferrites as gas sensor materials. J. Mater.Sci.Lett. 2000;19(9):775-778. DOI: 10.1023/A:1006716721984

9. Dube GR and Darshane VS.Decomposition of 1-octanol on the spinel system $Ga_{1-x}Fe_xCuMnO_4$. J. Molecular Catalysis. 1993;79(1):285. DOI: 10.1016/0304-5102(93)85108-6

10. Larumbe S, Perez-Landazabal JI, Pastor JM and Gomez-Polo C. Sol-gel $NiFe_2O_4$ nanoparticles: Effect of the silica coating. J. Appl. Phys. 2012;111(10):103911.

11. JacobsIS, BeanCP. Fine particles, thin films and exchange anisotropy. In: RadoGT, Suhl H, Editors. Magnetism.Vol. III; Academic Press; New York; 1963. p. 271-350.

12. ChantrellRW, O'Grady K. The Magnetic Properties of Fine Particles. In: Gerber Ret al., Editors. Applied Magnetism.Kluwer Academic; Dordrecht; Netherlands; 1994. p. 113-164.

13. Shi W, Zeng H, Sahoo Y, Ohulchanskyy TY, Ding Y, Wang ZL, et al.A general approach to binary and ternary hybrid nanocrystals. Nano Lett. 2006;6(4):875-881. DOI: 10.1021/nl0600833

14. B.B. Zhang, J.C. Xu, P.F. Wang, Y.B. Han, B. Hong, H.X. Jin, et al. Ordered $NiO/NiFe_2O_4$ nanocomposites: Synthesis, exchange bias and magnetic properties. J. Alloys Comp. 2016;662:348-354.

15. Miki J, Asanuma M, Tachibana Y andShikada T. Vapor Phase Oxidation of Benzoic Acid to Phenol over a Novel Catalyst System Consisting of NiO and $NiFe_2O_4$. J. Catalysis. 1995;151(2):323-329. doi:10.1006/jcat.1995.1034

16. Z. M. Tian, S. L. Yuan, S. Y. Yin, L. Liu, J. H. He, H. N. Duan, et al. Exchange bias effect in a granular system of $NiFe_2O_4$ nanoparticles embedded in an antiferromagnetic NiO matrix. Appl. Phys. Lett. 2008;93(22):222505.

17. Z M Tian, S L Yuan, L Liu, S Y Yin, L C Jia, P Li et al. Exchange bias training effect in $NiFe_2O_4$/NiO nanocomposites. J. Phys. D: Appl. Phys. 2009;42(3):035008.

18. J.H. He, S.L. Yuan, S.Y. Yin, K.L. Liu, P. Li, C.H. Wang, et al. Analysis of exchange bias effect of $NiO+NiFe_2O_4$ composites. J.Magn.Magn.Mater. 2010;322(1):79-83.

19. Zhao X, Xu S, Wang L, Duan X and Zhang F. Exchange-biased $NiFe_2O_4$/NiO nanocomposites derived from NiFe-layered double hydroxides as a single precursor. Nano Research. 2010;3(3):200-210. doi:10.1007/s12274-010-1023-3

20. Tian ZM, Chen JT, Yuan SL, Zhang YS, Ma ZZ, Duan HN, et al. Cooling field and temperature dependence on training effect in $NiFe_2O_4$-NiO nanogranular system. J. Appl. Phys. 2011;110(10):103902.

21. W. J. Gong, W. Liu, D. Li, S. Guo, X. H. Liu, J. N. Feng, et al. Exchange bias effect in $NiO/NiFe_2O_4$ nanocomposites. J. Appl. Phys. 2011;109(7):07D711.

22. Tian ZM, Huang S, Qiu Y, Yuan SL, Wu YY and Li L. Size-dependent scaling of exchange bias in $NiFe_2O_4$/NiOnanogranular systems synthesized by a phase separation method. J. Appl. Phys. 2013;113(14):143906.

23. Zhaoming Tian, Changming Zhu, Yong Liu, Zhongwen Ouyang, Jing Shi, Zhengcai Xia, et al. Size-dependent training effect in exchange coupled $NiFe_2O_4$/NiOnanogranular systems. J. Appl. Phys. 2014;115(8):083902.

24. Hadjipanayis GC. Nanophase hard magnets. J.Magn.Magn.Mater. 1999;200(1):373-391.

25. Sort J, Nogués J, Amils X, Suriñach S, Muñoz JS and Baró MD. Room-temperature coercivity enhancement in mechanically alloyed antiferromagnetic-ferromagnetic powders.Appl. Phys. Lett. (1999);75: 3177.

26. J. Sort, J. Nogués, S. Suriñach, J. S. Muñoz, M. D. Baró, E. Chappel, et al. Coercivity and squareness enhancement in ball-milled hard magnetic-antiferromagnetic composites. Appl. Phys. Lett. 2001;79(8):1142.

27. Kodama RH. Magnetic nanoparticles. J.Magn.Magn.Mater. 1999;200(1):359.

28. Nogués J, Sort J, Langlais V, Skumryev V, Surinach S, Munoz JS, et al. Exchange bias in nanostructures. Phys. Rep. 2005;422(3):65.

29. YanqingL, HuananD, JieL, XiaogangS and Yexiang L. On the Corrosion Behaviour ff Ni-NiO-$NiFe_2O_4$Cermets as Inert Anodes in Aluminum Electrolysis. In: KvandeHalvor,Editor. Light Metals.The Minerals, Metals & Materials Society; 2005. p. 529-534.

30. Morozov YG, Belousova OV and Kuznetsov MV. Preparation of nickel nanoparticles for catalytic applications. Inorganic Mater. 2011;47(1):36-40. DOI: 10.1134/S0020168510121027

31. Kuznetsov MV, Morozov YG and Belousova OV. Levitation jet synthesis of nickel ferrite nanoparticles.Inorganic Mater. 2012;48(10):1044-1051. DOI: 10.1134/S0020168512100020

32. Ma Li, Zhou K, Li Z, Wei Q and Zhang L. Hot corrosion of a novel NiO/$NiFe_2O_4$ composite coating thermally converted from the electroplated Ni–Fe alloy. Corrosion Sci. 2011;53(11):3712-3724.

33. Pebley AC, Peek A, Pollock TM and Gordon MJ. Microplasma-Based Growth of Biphasic $NiFe_2O_4$/NiONanogranular Films for Exchange Bias Applications. Chem. Mater. 2014;26(20):6026.

34. Zhang Y, Zhang F, Lu Y, Chen T and Yang L. Preparation and characterization of $NiFe_2O_4$/NiO composite film via a single-source precursor route. J. Phys. Chem. Solids. 2010;71(4):604-607.

35. Šepelák V, Ingo Bergmann, Armin Feldhoff, Paul Heitjans, Frank Krumeich, Dirk Menzel, et al. Nanocrystalline nickel ferrite, $NiFe_2O_4$: mechanosynthesis, nonequilibrium cation distribution, canted spin arrangement, and magnetic behavior. J. Phys. Chem. C. 2007;111(13):5026-5033. DOI: 10.1021/jp067620s

36. Pettigrew KA, Long JW, Carpenter EE, Baker CC, Lytle JC, Chervin CN, et al. Nickel Ferrite Aerogels with Monodisperse Nanoscale Building Blocks: The Importance of Processing Temperature and Atmosphere. ACS Nano. 2008;2(4):784-790. doi: 10.1021/nn7002822.

37. Mumtaz A, Maaz K, Janjua B, Hasanain SK and Bertino MF. Exchange bias and vertical shift in $CoFe_2O_4$ nanoparticles. J.Magn.Magn.Mater. 2007;313(2):266-272. DOI: 10.1016/j.jmmm.2007.01.007

38. Feygenson M, Yiu Y, Kou A, Kim KS and Aronson MC. Controlling the exchange bias field in Co core/CoO shell nanoparticles. Phys. Rev. B. 2010;81(19):195445.

39. Meiklejohn WH and Bean CP. New magnetic anisotropy. Phys. Rev. 1956;102(5):1413.

40. Berkowitz AE and Takano K. Exchange anisotropy—a review. J. Magn. Magn.Mater. 1999;200(1):552.

41. Kavich DW, Dickerson JH, Mahajan SV, Hasan SA and Park JH. Exchange bias of singly inverted $FeO/Fe_3O_4$ core-shell nanocrystals. Phys. Rev. B. 2008;78(17):174414.

42. Del Bianco L, Fiorani D, Testa AM, Bonetti E and Signorini L. Field-cooling dependence of exchange bias in a granular system of Fe nanoparticles embedded in an Fe oxide matrix. Phys. Rev. B. 2004;70(5):052401.

43. Ali M, Adie P, Marrows CH, Greig D, Hickey BJ and Stamps RL. Exchange bias using a spin glass. Nature Mater. 2007;6(1):70-75. DOI: 10.1038/nmat1809

44. Kodama RH, Makhlouf SA and Berkowitz AE. Finite size effects in antiferromagnetic NiO nanoparticles. Phys. Rev. Lett. 1997;79(7):1393.

45. Skumryev V, Stoyanov S, Zhang Y, Hadjipanayis G, Givord D and Nogues J. Beating the superparamagnetic limit with exchange bias. Nature. 2003;423(6942):850-853. DOI: 10.1038/nature01687

46. Liu XH, Cui WB, Lv XK, Liu W, Zhao XG, Li D and Zhang ZD. Exchange bias and phase transformation in $\alpha Fe_2O_3$+ NiO nanocomposites. J. Appl. Phys. (2008);103:103906. DOI:10.1063/1.2927458

47. Ioannis Panagiotopoulos, Georgia Basina, Vassilios Alexandrakis, Eammon Devlin, George Hadjipanayis, Levent Colak, et al. Synthesis and Exchange Bias in $\gamma$-$Fe_2O_3$/CoO and Reverse CoO/$\gamma$-$Fe_2O_3$ Binary Nanoparticles. J. Phys. Chem. C. 2009;113(33):14609-14614. DOI: 10.1021/jp8085446

48. Binek C. Training of the exchange-bias effect: A simple analytic approach. Phys. Rev. B. 2004;70(1):014421.

49. Binek C, He X andPolisetty S. Temperature dependence of the training effect in a Co/ CoO exchange-bias layer. Phys. Rev. B. 2005;72(5):054408.

50. Paul A, Schneider CM and Stahn J. Reversal mechanism and suppression of training in an exchange-coupled system. Phys. Rev. B. 2007;76(18):184424. DOI: 10.1103/PhysRevB.76.184424

51. Leighton C, Nogués J, Jönsson-Åkerman BJ and Schuller IK. Coercivity enhancement in exchange biased systems driven by interfacial magnetic frustration. Phys. Rev.Lett. 2000;84(15):3466-3469. DOI: 10.1103/PhysRevLett.84.3466

52. Padhan P andPrellier W. Coercivity enhancement in the $SrRuO_3$/ $SrMnO_3$superlattices. Appl. Phys.Lett. 2006;88:263114. DOI: 10.1063/1.2217187

53. CullityBD,Stock SR. Elements of X-Ray Diffraction.3rd Ed. Prentice-Hall Inc.; 2001.

54. NeelL. Low Temperature Physics.In: DewittC, DreyfusB and de GennesPD,Editors.Gordon and Breach; New York; 1962.p. 413.

55. Winkler E, Zysler RD, Mansilla MV and Fiorani D. Surface anisotropy effects in NiO nanoparticles. Phys. Rev. B. 2005;72(13):132409.

56. Winkler E, Zysler RD, Mansilla MV, Fiorani D, Rinaldi D, Vasilakaki M andTrohidou KN. Surface spin-glass freezing in interacting core–shell NiO nanoparticles. Nanotechnol. 2008;19(18):185702.

57. Kodama RH and Berkowitz AE. Atomic-scale magnetic modeling of oxide nanoparticles. Phys. Rev. B. 1999;59(9):6321.

58. Nowak U, Usadel KD, Keller J, Miltényi P, Beschoten B and Güntherodt G. Domain state model for exchange bias. I. Theory. Phys.Rev. B. 2002;66(1):014430.

59. Del Bianco L, Boscherini F, Fiorini AL, Tamisari M, Spizzo F, Antisari MV and Piscopiello E. Exchange bias and structural disorder in the nanogranularNi/NiO system produced by ball milling and hydrogen reduction. Phys. Rev. B. 2008;77(9):094408.

60. Tang YK, Sun Y and Cheng ZH. Exchange bias associated with phase separation in the perovskite cobaltite $La_{1-x}Sr_xCoO_3$. Phys. Rev. B. 2006;73(17):174419. DOI:10.1103/PhysRevB.73.174419

61. J. H. He, S. L. Yuan, Y. S. Yin, Z. M. Tian, P. Li, Y. Q. Wang, et al. Exchange bias and the origin of room-temperature ferromagnetism in Fe-doped NiO bulk samples. J. Appl. Phys. 2008;103(2):023906.

62. Vallejo-Fernandez G, Fernandez-Outon LE and O'Grady K. Antiferromagnetic grain volume effects in metallic polycrystalline exchange bias systems. J. Phys. D: Appl. Phys. 2008;41(11):112001.

63. Kodama RH, Berkowitz AE, McNiff Jr EJ and Foner S. Surface spin disorder in $NiFe_2O_4$ nanoparticles. Phys. Rev. Lett. 1996;77(2):394-397. DOI: 10.1103/PhysRevLett.77.394